In: IET Radar 2022: International Conference on Radar Systems, 24-27 October 2022, Edinburgh, Scotland
DOI:10.1049/icp.2022.2294; https://ieeexplore.ieee.org/document/10038928

MULTISTATIC HYBRID SAR/ISAR DATA GENERATION USING A STATIONARY TARGET

Anmol Rattan[1*], Daniel Andre[1], Mark Finnis[2]

[1]Centre for Electronic Warfare Information and Cyber, Cranfield University, Defence Academy of the United Kingdom, Shrivenham, UK
[2]Centre for Defence Engineering, Cranfield University, Defence Academy of the United Kingdom, Shrivenham, UK
** Anmol.Rattan@cranfield.ac.uk*

Keywords: MULTISTATIC, HYBRID SAR/ISAR, SIX-DEGREES-OF-FREEDOM MOTION, MOTION ESTIMATION

Abstract

There is great interest in multistatic synthetic aperture radar (SAR) systems as they are capable of providing high resolution images. These systems could prove promising candidates for provision of surveillance for both military and civilian interest. Both multistatic SAR and its counterpart, multistatic inverse synthetic aperture radar (ISAR), are limited by their assumptions of observing a stationary target from a moving platform and vice-versa. Hence, without adequate target motion compensation, their resultant radar images appear defocused. Arranging experiments capable of providing repeatable multistatic hybrid SAR/ISAR data of real moving targets can be difficult and costly. One viable approach is the novel method presented in this study, whereby multistatic hybrid SAR/ISAR data can be collected of a target moving with a theoretical motion, without the requirement of an actual moving target – the theoretical motion is brought about through the appropriate motion of antennas. The study demonstrates, both through simulation and experimentation, how radar trajectories of a given SAR system can be altered to arrive at the equivalent setup of observing a moving target. Results from simulation and from an experiment conducted at the Cranfield University Ground-Based SAR (GBSAR) laboratory are presented, showing the utility of this approach.

1 Introduction

Multistatic synthetic aperture radar (SAR) systems make it possible to acquire high-resolution images whilst utilising low cost, covert and passive receivers in the mix of radar platforms. However, the basic theory of SAR assumes that the scene or target being imaged is stationary. Ships are one type of noncooperative target whose identification is of great interest for both military and civilian applications. Generally, both the SAR system and ships are in a state of motion. The defocusing effect on resultant SAR images is often proportional to the magnitude of the target motion; focusing these images becomes even more difficult when the nature of the motion is unknown.

Hybrid SAR/ISAR techniques make it possible to utilise the advantages of both SAR and ISAR to help disentangle the dilemma of motion compensation; one such technique is focusing a moving target using ISAR processing prior to SAR image formation [1], which has been incorporated in this study. Understanding the effects of target motion on SAR/ISAR imaging is a vital step towards building improved future multistatic hybrid SAR/ISAR systems which could potentially predict the motions of certain targets and help identify them with ease, for example by allowing three-dimensional (3D) target reconstruction [2][3]. Setting up experiments for realistic hybrid SAR/ISAR scenarios, however, can be difficult given that one requires a moving target, normally of controlled motion, in order to produce repeatable results.

In efforts to solve this problem, this study presents a novel method which allows the collection of radar data of a target with a theoretical motion of up to 6 Degrees-of-Freedom (DoF) during a multistatic SAR collection, without requiring the target to actually move. The practicality of this method is demonstrated using ground-based synthetic aperture radar (GBSAR), which is highly regarded for its accurate repeatability and flexibility in testing many SAR configurations [4][5][6]. Section 2 expands upon the method by introducing the multistatic radar system and scene used to obtain simulated and experimental results in this study and the hybrid SAR/ISAR conceptualisation behind this method. The same method has been shown to assist with motion compensation and generation of focused SAR images, which are presented and discussed in Section 3.

2 Methodology

2.1 Multistatic Radar System and Scene

This study implements simulation and experimental work. Experimental findings in this study utilise the Cranfield University Ground-Based SAR laboratory system; see Fig. 1. Using a given bistatic configuration, this system is able to gather high resolution SAR data by using a Vector Network Analyser (VNA) connected to receiver and transmitter Ultra-Wideband horn antennae. The receiver and transmitter can transverse in separate vertical planes of motion and are controlled via two, two-dimensional (2D) scanners. Each scanner is mounted onto a railing which governs the aperture extent of an antenna. The transmitter railing allows its mounted scanning system to move across an aperture 3.5 m wide and 1.45 m tall, while the receiver railing allows for an aperture almost 1.3 m wide and 1.45 m tall – both providing 2D SAR apertures individually, and four-dimensional (4D) motion when considered jointly.

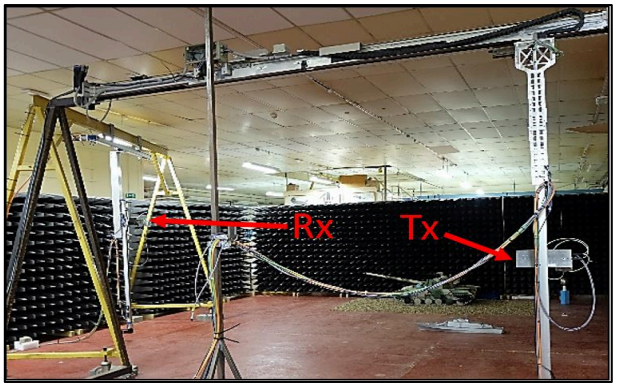

Fig. 1: Cranfield University GBSAR Laboratory System

Fig. 2 demonstrates the initial multistatic radar configuration and target scene for all data gathering in this study. The scene size measures approximately 4 m parallel to the transmitter railing (or along the x-axis) and 8 m along the y-axis. The multistatic radar geometry utilised here is composed of three individual bistatic geometries; each individual bistatic geometry has a stationary receiver at one of three heights, whilst receiving from the same transmitter trajectory which travels along a straight flight path of aperture ~3.2 m. In practice, the laboratory system only has a single receiver, however if the experimental conditions are precisely repeated, with the receiver at a different location (or trajectory), then the combination of collections are equivalent to a single multiple receiver multistatic collection. An eventual goal is to form 3D SAR imagery via the multiple bistatic collections which comprise a multistatic collection.

The bistatic equivalent monostatic (BEM) radar trajectories, are defined here as the collection of points that lie half-way between the transmitter and receiver positions. For the utilised multistatic SAR geometry, the BEM radar trajectories therefore provide an aperture of 1.6 m for each bistatic case. Data was both simulated and experimentally gathered over the frequency band 11-18 GHz, corresponding to a bandwidth of 7 GHz and a central frequency of 14.5 GHz. A range of bistatic angles are produced during each bistatic case due to transmitter movement; average bistatic angles of all three bistatic cases were quite similar to one another (69.1° ±1.2°). This gave a theoretical average bistatic range resolution of ~2.6 cm and average bistatic cross range resolution of ~1.7 cm for each bistatic case at a range of ~4.2 m at the target centre.

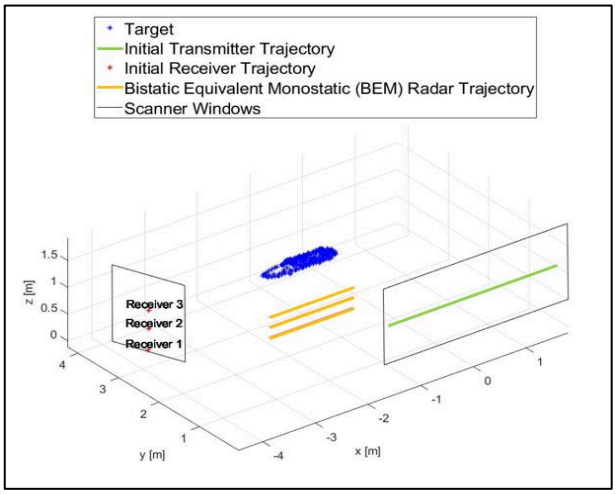

Fig. 2: Initial Multistatic SAR Geometry and Target Scene

Fig. 3 (a) displays the ship model used in simulation work. Whilst this simulated model is not an exact version of the ship model used in the laboratory experiment, seen in Fig. 3 (b), it has been dimensioned to match the size of the real ship model; its dimensions are 1.35 m ⨯ 0.23 m ⨯ 0.2 m (L x W x D).

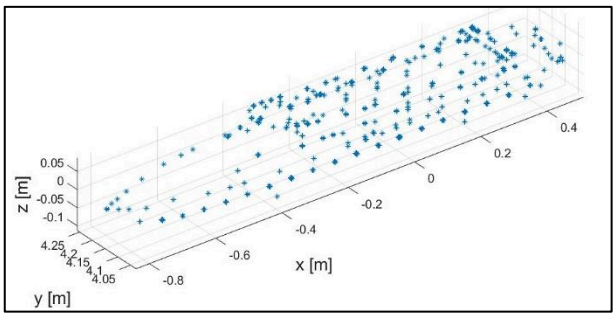

a

b

Fig. 3: (a) Point-Scatterer Ship Model used in Simulation and (b) Real Ship Model used in Laboratory Experiment

2.2 Initial Signal Model

For the initial multistatic radar configuration seen in Fig. 2, the transmitter travels along its flight path in 3D space such that its spatial location can be defined as:

$$\underline{T_R}(\tau) = \left[T_{Rx}(\tau), T_{Ry}(\tau), T_{Rz}(\tau)\right] \quad (1)$$

where τ is the slow time parameter.

Similarly, the three receivers are located in 3D space as:

$$\underline{R_{Rn}}(\tau) = \left[R_{Rxn}(\tau), R_{Ryn}(\tau), R_{Rzn}(\tau)\right] \quad (2)$$

where n denotes the receiver number $\{n = 1,2,3\}$.

The ship model consists of m scatterers which could have any arbitrary motion. Their 3D coordinates are defined as:

$$\underline{P_m}(\tau) = \left[p_{xm}(\tau), p_{ym}(\tau), p_{zm}(\tau)\right] \quad (3)$$

This study utilised the back-projection algorithm (BPA) [7], but extended to the bistatic case. The BPA provides accurate results, both in the SAR far-field and near-field regimes. For K frequency samples per pulse and N_p pulses used to form an image, the signal return of a single target scatterer with a reflectivity $A_{(f_k,\tau_n)}$ is:

$$S_{m(f_k,\tau_n)} = A_{m(f_k,\tau_n)} e^{\left(\frac{-i4\pi f_k d_{TP}(\tau)}{c}\right)} \quad (4)$$

where f_k represents specific values within the frequency sample $\{f_k | k = 1,2,\dots,K\}$, τ_n signifies the transmission time for each pulse $\{\tau_n | n = 1,2,\dots,N_p\}$, $d_{TP}(\tau)$ is half the distance covered by each pulse on its journey from the transmitter to a given receiver after being reflected by target scatterers, and c is the speed of light.

Superposition of signal returns by all observed target scatterers results in the full signal as:

$$S_{(f_k,\tau_n)} = \sum_m S_{m(f_k,\tau_n)} \quad (5)$$

This signal, however, is affected by target motion which needs to be compensated before a focused SAR image can be obtained.

2.3 Hybrid SAR/ISAR Target Motion Compensation

Based on 6-DoF motion, the motion of a target ship can be classified under two categories: linear and angular oscillations. As defined in [8] for ships, linear oscillations are translational motions along three axes, while angular oscillations are rotations about those three axes. Fig. 4 helps visualise these motions.

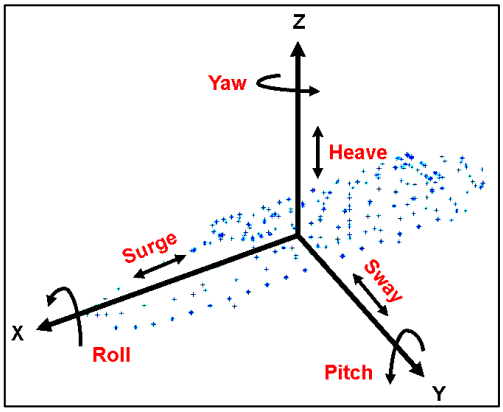

Fig. 4: 6-DoF Ship Motion Geometry

Linear oscillations of ships along their longitudinal axis (x axis), transverse axis (y axis) and vertical axis (z axis) are called surge, sway and heave respectively. Real motion parameters of ships are complicated due to their time-varying and approximately sinusoidal nature, and the overall motion is typically viewed as the superposition of the 6-DoF multi-frequency motion [9]. Therefore, this study began by simplifying the linear and angular oscillations of a ship to shifts and fixed angle rotations respectively.

For a given set of target scatterers in 3D space $\underline{P_m}(\tau)$, their final coordinates $\underline{P_{m(final)}}(\tau)$ following shifts and rotations can be defined as:

$$\underline{P_{m(final)}}(\tau) = \underline{\underline{R_1}} \left(\underline{P_m}(\tau) - \underline{r_{shift}} \right) \quad (6)$$

where $\underline{r_{shift}}$ represents shifts along all three axes and $\underline{\underline{R_1}}$ is a rotation matrix representing rotations about all three axes by angles θ_x , θ_y and θ_z:

$$\underline{\underline{R_1}} = \underline{R_{z(\theta_z)}}\, \underline{R_{y(\theta_y)}}\, \underline{R_{x(\theta_x)}} \quad (7)$$

If this target motion is estimated or known, it can be realised that in order to compensate this motion, the bistatic radar trajectory during SAR processing could be altered to move inversely to the 6-DoF target motion. For the transmitter positions, this is:

$$\underline{T_{R(final)}}(\tau) = \left(\underline{\underline{R_1}}^{-1}\, \underline{T_R}(\tau) \right) + \underline{r_{shift}} \quad (8)$$

And for the receiver positions, this is:

$$\underline{R_{R(final)}}(\tau) = \left(\underline{\underline{R_1}}^{-1}\, \underline{R_R}(\tau) \right) + \underline{r_{shift}} \quad (9)$$

2.4 Hybrid SAR/ISAR Measurements using a Stationary Target

Based upon the motion compensation technique described in Section 2.3, one can begin with a stationary target, invert the radar trajectory by the inverse of a desired target motion and effectively attain the equivalent data that one would observe from a theoretical movement of this target during a SAR data collection.

To put this theory into practice, this study conducted both simulation and experimental work, the latter providing practical validation. Steps undertaken are explained below and also summarised by a flowchart seen in Fig. 5.

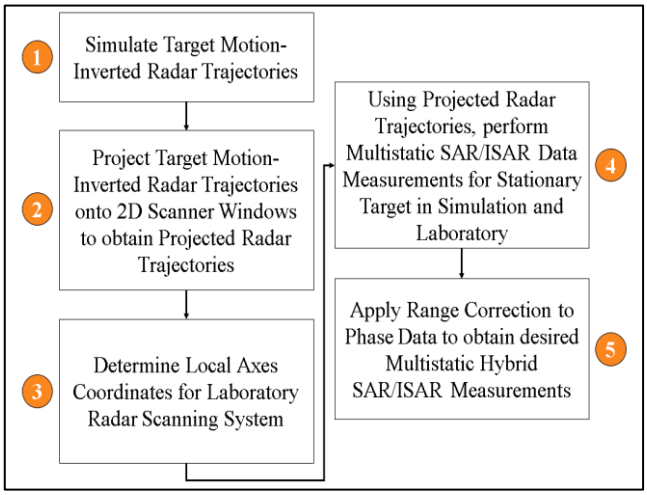

Fig. 5: Methodology of Hybrid SAR/ISAR Data Collection Using a Stationary Target

Table 1 details a case of 6-DoF target motion that was investigated for this method of hybrid SAR/ISAR data collection.

Table 1: Investigated 6-DoF Target Motion Case

Target Motion	$Shift_x$	$Shift_y$	$Shift_z$	θ_x	θ_y	θ_z
	$0.2\,m$	$0.2\,m$	$0.2\,m$	$-3°$	$-3°$	$-3°$

Investigating this set of 6-DoF target motion values was deemed possible following a test simulation. Each scanner within the laboratory is mounted onto a railing, which confines antenna movement to a 2D window. In reality, inverting the radar trajectories shown in Fig. 2 by a given magnitude of 6-DoF motion is bound to place the resultant radar trajectories outside the 2D extents of the scanner windows. Therefore, to obtain target motion-inverted radar trajectories which could feasibly be carried out in the laboratory, the process began by simulating the radar and target scene shown in Fig. 2, and the following steps implemented:

1. Using (8) and (9) – a set of three target motion-inverted bistatic radar trajectories were computed. Existing outside the 2D extents of each scanner window, the radar trajectories were not physically attainable by the scanner system;
2. To overcome this issue, the target motion-inverted radar trajectories were projected onto their respective 2D scanner windows along a chord joining the target centre with a given trajectory position. In turn, the target motion-inverted radar trajectories underwent range corrections (R_{Cn}) to produce the projected radar trajectories.
3. 3D coordinates of the projected radar trajectories were converted to local antenna axes coordinates as inputs for the laboratory scanning system for measurement;
4. Using the projected radar trajectories and stationary ship models seen in Fig. 3, multistatic hybrid SAR/ISAR data measurements were made in simulation and the laboratory;
5. The acquired phase data measurements were multiplied by a phase ramp term ($e^{(-i4\pi f_k R_{Cn}/c)}$) to achieve the desired phase data – as if measured using the target motion-inverted radar trajectories. This was done for both simulated and experimental phase data measurements for comparison.

2.5 6-DoF Target Motion Compensation and Image Formation

Supposing three phase data collections have been obtained during SAR scans without use of any prior knowledge of the target motion (let alone the target motion-inverted trajectories), each phase data collection must now be motion compensated before any SAR image formation. As mentioned in Section 2.2, image formation was performed using the back-projection algorithm [7] extended to the bistatic case.

Target motion compensation was conducted using a similar procedure to that described in Section 2.3, whereby a collection of target motion-inverted radar trajectories were hypothesised, relating to different magnitudes of 6-DoF motion, with the aim of obtaining optimally focused SAR imagery with one of these radar trajectories. During these iterative searches, image quality measures such as image contrast [10] and entropy [11] were employed and calculated of SAR images for each receiver. Extending this to a multistatic case, image contrast values relating to SAR images by each of the three receivers in the multistatic configuration were multiplied with each other for each iteration; the same was done with the entropy values to produce product compositions of individual image contrast and entropy values. This was done to jointly consider hybrid SAR/ISAR image contributions resulting from all receivers in the multistatic radar system [10]. Indexes of maximum image contrast product and minimum entropy product values were utilised to determine which hypothetical target motion-inverted radar

trajectories to use for the formation of optimally focused SAR imagery. Usage of image contrast and entropy products like this has been justified in [12]. However, the comparability of hybrid SAR/ISAR images from all receivers in a multistatic radar system like this may be limited to cases where the average bistatic angles of all bistatic cases are not vastly different to each other, or where the height difference between the bistatic radar trajectories is under a certain threshold, such that the target reflectivity and shadowing realised across the bistatic hybrid SAR/ISAR images is not significantly different.

3 Results

3.1 Hybrid SAR/ISAR Images

Fig. 6 (a) and (b) show 2D unfocused and focused hybrid SAR/ISAR images acquired via simulation from Receiver 1. Focused images formed from all receivers shared close resemblance to each other, therefore only images from Receiver 1 have been shown. Likewise, Fig. 7 (a) and (b) show 2D unfocused and focused hybrid SAR/ISAR images produced using experimental data from Receiver 1. It is emphasised that the focused images here, were obtained via an iterative search of hypothesised target motions. Note that the maximum image contrast product and minimum entropy product values were found to agree on the same hypothetical target motion-inverted radar trajectories to produce optimally focused SAR imagery for simulation and experimental results respectively.

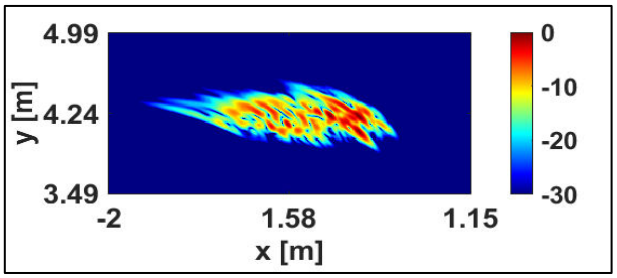

a

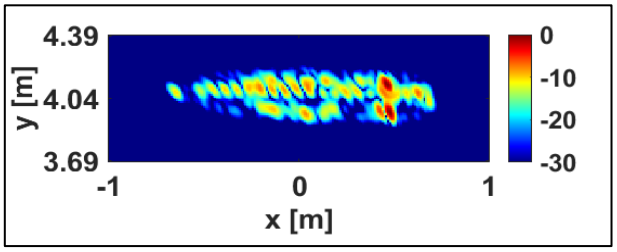

b

Fig. 6: Simulation Results showing (a) Unfocused and (b) Focused 2D Hybrid SAR/ISAR Images from Receiver 1

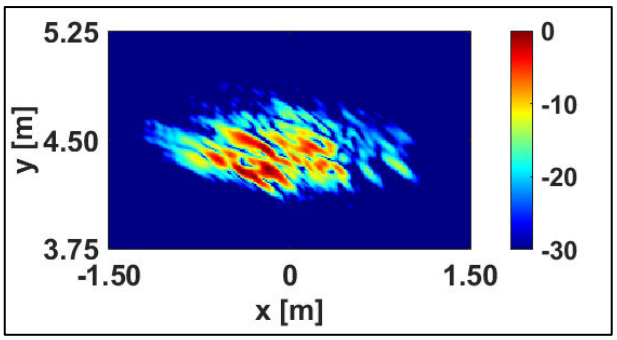

a

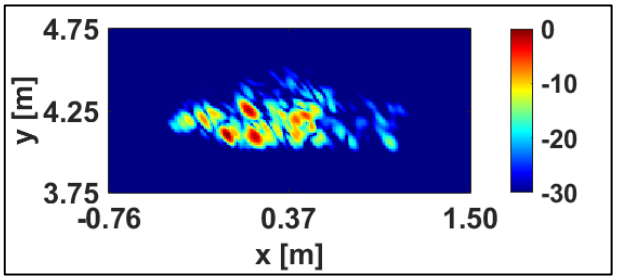

b

Fig. 7: Experimental Results showing (a) Unfocused and (b) Focused 2D Hybrid SAR/ISAR Images from Receiver 1

For both simulated and experimental data, Fig. 8 (a) and (b) show focused 2D hybrid SAR/ISAR images which have been formed using prior knowledge of target motion, referred to here as the 'hidden target motion information'.

Images focused without hidden target motion information show evidence of successful motion compensation, as the general shape of the ship models is apparent, target features are clearer and smearing is substantially less than the unfocused images. Furthermore, they compare very well with focused images produced using the hidden target motion information. Normalised cross-correlation results between the two set of focused images (focused with and without the use of hidden target motion information) seen in Table 2 help quantify and corroborate the likeness of the focused images; a result of one represents complete similarity, whereas a result of zero reflects complete dissimilarity. Based on this definition, results within Table 2 report a strong resemblance between the two sets of focused images for both simulated and experimental data.

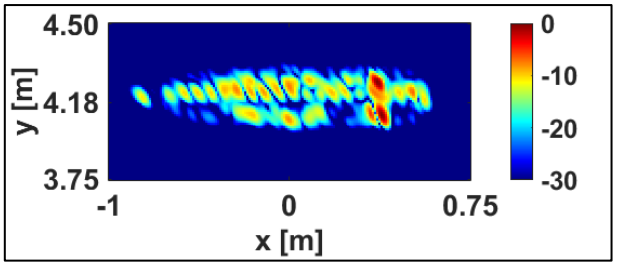

a

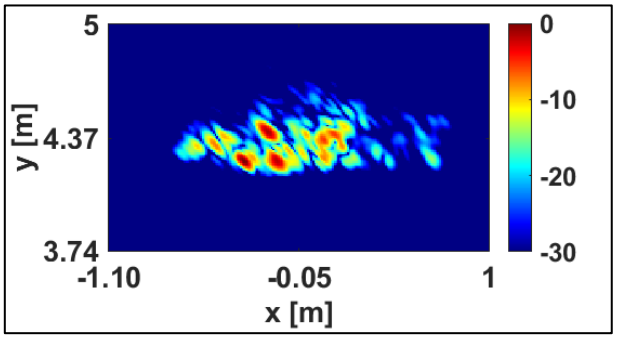

b

Fig. 8: Focused 2D Hybrid SAR/ISAR images formed with hidden target motion information using (a) Simulated Data and (b) Experimental Data from Receiver 1

Table 2: Normalised cross-correlation between images focused with and without hidden target motion information

Simulation	Experimentation
0.975	0.962

4 Conclusion

This study has presented a new method for collecting hybrid multistatic SAR/ISAR data of a target with a theoretical motion without the necessity of having an actual moving target during the radar data measurement. Results have demonstrated that up to 6-DoF target motion can be emulated by inverting the radar antenna trajectories accordingly.

The same approach can be adjusted to incorporate a hybrid SAR/ISAR method of motion compensation, estimating the motion parameters of the target and producing focused SAR images.

This study has demonstrated the ability of obtaining hybrid multistatic SAR/ISAR measurements of a target moving with 6-DoF motion without the need of an actual moving target and an elaborate radar setup. In turn, the method discussed in this study may offer an easier and cost-effective alternative of gathering experimental data to research the effects of target motion on multistatic SAR imagery, one which extends to how this target motion could also be compensated.

Future work will centre around expanding this method to 3D hybrid multistatic SAR/ISAR imaging, by jointly using the data from multiple receivers in a multistatic collection, and investigating more efficient techniques of motion estimation and compensation which require fewer iterative searches. Polarimetric features will also be investigated.

5 Acknowledgements

The authors would like to thank the Defence Science and Technology Laboratory (Dstl) for funding this study.

6 References

[1] Martorella, M., Berizzi, F., Giusti, E., Bacci, A.: 'Refocusing of moving targets in SAR images based on inversion mapping and ISAR processing', IEEE 2011 Radar Conference, 2011.

[2] Chen, V.C., Liu, B.: 'Hybrid SAR/ISAR for distributed ISAR imaging of moving targets', IEEE Radar Conference (RadarCon), 2015, pp. 0658-0663

[3] Salvetti F., Giusti E., Staglianò D. et al.: 'Multistatic 3D ISAR image reconstruction'. 2015 IEEE Radar Conf. (RadarCon), Washington DC, USA, May 2015, pp. 0640 – 0645

[4] Lee, H., Moon, J.: 'Indoor Experiments of Bistatic/Multistatic GB-SAR with One-Stationary and One-Moving Antennae', Remote Sens, 2021, 13, (18), pp. 3733

[5] Corbett, B., Andre, D., Finnis, M.: 'Localising vibrating scatterer phenomena in synthetic aperture radar imagery', Electron. Lett., 2020, 56, pp. 395-398

[6] Elgy, J., Andre, D., Finnis, M.: 'Volumetric SAR near-field upsampling and basebanding', Electron. Lett., 2020, 56, pp. 622-624

[7] Gorham, L.A., Moore, L.J.: 'SAR image formation toolbox for MATLAB', Proc. SPIE 7699, Algorithms for Synthetic Aperture Radar Imagery XVII, 2010, 769906

[8] Zhou, B., Qi, X., Zhang, J. et al.: 'Effect of 6-DOF Oscillation of Ship Target on SAR Imaging', Remote Sens, 2021, 13, (9), pp. 1821

[9] Yao, G., Xie, J., Huang, W.: 'HF Radar Ocean Surface Cross Section for the Case of Floating Platform Incorporating a Six-DOF Oscillation Motion Model', IEEE Journal of Oceanic Engineering, 2021, 46, (1), pp. 156-171

[10] Brisken, S., Martorella, M., Mathy, T. et al.: 'Multistatic isar autofocussing using image contrast optimization', IET International Conference on Radar Systems, 2012, pp. 1-4

[11] Shin, S.Y., Myung, N.H.: 'The application of motion compensation of ISAR image for a moving target in radar target recognition', Microwave and Optical Technology Letters, 2008, 50, (6), pp. 1673–1678

[12] Brisken, S., Martorella, M.: 'Examination of cost functions for multistatic image quality based autofocus', 2013 Signal Processing Symposium (SPS), 2013, pp. 1-4